Interval Type-2 and General Type-2 Possibilistic Fuzzy-C-Means

Michael Shell, *Member, IEEE,* John Doe, *Fellow, OSA,* and Jane Doe, *Life Fellow, IEEE*

Abstract

Possibilistic fuzzy-c-means (PFCM) was introduced to solve problems of unsupervised clustering by eliminating the drawbacks of previously established algorithms of fuzzy-c-means (FCM), possibilistic-c-means (PCM) and fuzzy-possibilistic-c-means (FPCM). PFCM model, a hybridization of FCM and PCM, produces both membership values and possibility values simultaneously in addition to the cluster prototypes for each cluster. The PFCM model uses a fuzzifier denoted by m and a bandwidth parameter denoted by η which is used to evaluate the memberships and possibilities for fuzzy sets. However, when we consider fuzzy sets and assign fuzzy memberships and possibilities to a pattern set, there arises a question of uncertainty in the various parameters of Type-1 PFCM (T1-PFCM). In this paper, we extrapolate PFCM to interval type 2 fuzzy sets (IT2-PFCM) and general type-2 fuzzy sets (GT2-PFCM) by accounting for the uncertainty in the fuzzifier m and bandwidth parameter, η by incorporating an interval of the possible fuzzifier m lying between m_1 and m_2 and an interval of the possible bandwidth parameter η lying between η_1 and η_2, which creates a footprint of uncertainty(FOU) for m and η. The extra degree of freedom in type-2 fuzzy sets makes type-2 PFCM outperform type-1 PFCM. Type-reduction and defuzzification is then performed to result in the final desired clusters. Several numerical examples are given to show the validity of T2-PFCM by comparing the results with those of FCM, PCM, FPCM and T1-PFCM.

Index Terms

Possibilistic fuzzy-c-means(PFCM), interval type-2 PFCM, general type-2 PFCM, typicality values

I. Introduction

Clustering is the process of grouping similar entities together while taking into consideration some predefined features or attributes. In machine learning, one of the clustering techniques used is unsupervised learning, where, inferences are drawn from datasets consisting of input data without labelled responses[1]. While classical sets have crisp boundaries, in this paper, we deal with fuzzy sets, as first proposed by Zadeh in 1965 in [3] that account for even the inaccurate and ambiguous notions [2], and hence comes the concept of membership values. The membership values denote the degree with which an element x from the universe of discourse belongs to a particular set, where the membership value varies from 0 (not belonging to the set) to 1 (complete membership in the set). In other words, clustering can be thought of as two types, hard clustering and soft clustering. In hard clustering, the data points are divided into distinct sets, that is, a single data point can belong to only one cluster, whereas in soft clustering, data points have a fuzzy membership in a cluster, that is, a particular data point can belong to more than one cluster with different membership value [3]. While traditional hard clustering works for physical systems, fuzzy clustering is preferred for realistic human-centered systems.

Various algorithms have been previously introduced to solve unsupervised clustering problems for fuzzy sets. For our proposed algorithms, we discuss a few of these algorithms, namely, FCM, PCM and PFCM. FCM is the mostly widely used fuzzy clustering algorithm. FCM uses the concept of a fuzzifier m which is used to determine the membership value of a pattern x_k belonging to a particular cluster with cluster prototype, here the cluster center, v_i where k=1,2...n and i=1,2...c , where n is the number of patterns and c is the number of clusters. FCM requires the knowledge of the initial number of desired clusters and the membership value is decided by the relative distance between the pattern x_k) and the cluster center v_i . FCM finds its applications in classification of remote-sensing images[4], MRI image segmentation[5], tax administration[6], meteorological data[7], big data[] and tumor segmentation[8]. FCM has also been extended to Interval type-2[16] and general type-2 fuzzy sets[21]. However, one of the major drawbacks of using FCM is its noise sensitivity and constrained memberships and hence Possibilistic-C-Means (PCM) was introduced by Barni et al. in 1996.

PCM uses a parameter given by η whose value is estimated from the dataset itself. PCM applies the possibilistic approach which simply means that the membership value of a point in a class represents the typicality of the point in the class, or the possibility of the pattern x_k belonging to the class with cluster prototype v_i where k=1,2...n and i=1,2...c. Since, the noise points are comparatively less typical, while using typicality in PCM algorithm, the noise sensitivity is considerably reduced. PCM finds its applications in smartphones implementation [9], radar targets position acquisition [10], clustering incomplete multimedia data [11] and big data clustering [12]. PCM has further been extrapolated to Interval type-2 fuzzy sets in [17]. However, in PCM, clustering results are strongly dependent on parameter selection and initialization and the clustering accuracy is

M. Shell was with the Department of Electrical and Computer Engineering, Georgia Institute of Technology, Atlanta, GA, 30332 USA e-mail: (see http://www.michaelshell.org/contact.html).

J. Doe and J. Doe are with Anonymous University.

Manuscript received April 19, 2005; revised August 26, 2015.

affected due to the problem of coincident clustering [13]. To eliminate these drawbacks, fuzzy possibilistic-c-means clustering algorithm(FPCM) was introduced. FPCM generated both the memberships and possibilities simultaneously and solved the problem of noise sensitivity as seen in FCM and the coincident clusters as experienced in PCM[14].

However, in 2005, another algorithm, possibilistic fuzzy c means (PFCM) was introduced by Pal et al. which further solved the constraints of typicality values as seen in FPCM [15]. PFCM hybridizes FCM and PCM, where, the constraint on typicality values (or the constraint of row-sum=1) is relaxed but the column constraints on membership values is retained. PFCM uses the fuzzifier that is denoted by m, which determines the membership values, and the bandwidth parameter η that is used to evaluate the typicality values. PFCM further uses constants a and b that define the relative importance of fuzzy membership and typicality values in the objective function. Since PFCM utilizes more number of parameters to decide on the optimal solution for clustering, it provides an increased degree of freedom and hence renders better results as compared to the ones stated above. However, when we consider fuzzy sets and different parameters in a particular algorithm, we come across the possibility of the fuzziness of these parameters. In this paper, we account for the fuzziness in the possible value of the fuzzifier m and the bandwidth parameter η and generate a FOU for both by taking an interval of fuzziness for m, that is, considering the possibility of m lying in the interval m_1 and m_2, and an interval of fuzziness for η lying in the interval η_1 and η_2. This concept basically extrapolates the PFCM algorithm to type-2 fuzzy sets since it accounts for an extra degree of fuzziness called the secondary grade distribution of the fuzzifier m_1 and the parameter η. This type-2 PFCM (T1-PFCM) can either be taken as Interval type-2 PFCM (IT2-PFCM) or General type-2 PFCM (GT2-PFCM) depending on the distribution of secondary grade function in the interval between m_1 and m_2 and η_1 and η_2. If this secondary grade distribution is uniform over the interval, it is considered as IT2-PFCM and if the distribution is non-uniform then it is considered to be GT2-PFCM. The rest of the paper is organized as follows. Section II discusses Type 2 FCM, Type 2 PCM and T1-PFCM. In Section III we present the new IT2-PFCM and GT2-PFCM model. Section IV includes some the experimental examples that compare FCM, PCM,PFCM with our proposed IT2-PFCM and GT2-PFCM. Section V contains the conclusions.

II. Background

A. Type-1 Possibilistic Fuzzy-C-Means

As mentioned above, one of the most widely used algorithms for unsupervised clustering is FCM. However, FCM uses the concept of membership values of the pattern x_k belonging to the cluster with cluster prototype given by v_i, where k=1,2...n and i=1,2...c, with n being the number of data points and c is the number of desired clusters. The membership values depend on the fuzzifier given by m and the relative distance between the pattern and cluster center. Thus for a point x_j lying at equal distances from say, 2 cluster centers, the membership value of the pattern belonging to each of these clusters is 0.5, irrespective of its actual distance from the centroids. This leads to the problem of noise sensitivity, because in case of the distance being large, it actually should have close to zero membership in either of the clusters. To solve this problem of noise sensitivity, another variation of FCM was introduced in which the focus was shifted from the membership values to the typicality values, and this algorithm is called PCM. PCM, however, shows dependency on initialization and can sometimes generate coincident clusters. In 2005, Pal et al. came up with the PFCM algorithm for type-1 fuzzy sets which overcomes the above drawbacks and is a hybridization of FCM and PCM [15]. In PFCM, the constraint (row-sum=1) was relaxed on typicality values but retain the column constraint on membership values.

In, PFCM, the following optimization equation is used:

$$\min_{(U,T,V)} J_{m,\eta}(U,T,V;X) = \sum_{k=1}^{n}\sum_{i=1}^{c}(au_{ik}^{m} + bt_{ik}^{\eta}) \times \|x_k - v_i\|_A^2 + \sum_{i=1}^{c}\gamma_i \sum_{k=1}^{n}(1-t_{ik})^{\eta} \tag{1}$$

Subject to the constraints:

$$\sum_{i=1}^{c} u_{ik} = 1 \forall k = 1, 2...n \tag{2}$$

and,

$$0 \leq u_{ik}, t_{ik} \leq 1 \tag{3}$$

Here, $a > 0$,$b > 0$, $m > 1$ and $\eta > 1$. In (1), $\gamma_i > 0$ is a user-defined constant. The constants a and b define the relative importance of fuzzy membership and typicality values in the objective function.

In (1), the membership matrix U of the order $c \times n$, with the elements u_{ik} is given by the equation:

$$u_{ik} = (\sum_{j=1}^{c}(D_{ikA}/D_{jkA})^{2/(m-1)})^{-1} \tag{4}$$

where, $1 \leq k \leq n; 1 \leq i \leq c$

In (4),

$$D_{ikA} = \|x_k - v_i\|_A > 0 \quad \forall i;\ k, m, \eta > 1 \tag{5}$$

and,

$$\|x\|_A = \sqrt{x^t A x} \tag{6}$$

Similarly, the typicality matrix, T of the order $c \times n$ with elements given by t_{ik}:

$$t_{ik} = (1 + (b\frac{D_{ikA}^2}{\gamma_i})^{1/(\eta-1)})^{-1} \quad 1 \leq i \leq c;\ 1 \leq k \leq n \tag{7}$$

where,

$$\gamma_i = K\frac{\sum_{k=1}^{n} u_{ik} d_{ik}^2}{\sum_{k=1}^{n} u_{ik}} \tag{8}$$

The set of cluster centroids denoted in (1) by V consists of elements given by v_i :

$$v_i = \frac{\sum_{k=1}^{n}(au_{ik}^m + bt_{ik}^\eta)x_k}{\sum_{k=1}^{n}(au_{ik}^m + bt_{ik}^\eta)} \tag{9}$$

Fuzzy sets were introduced to cater to the uncertainties as seen in real-life applications as opposed to the application of the classical notion of sets for physical systems. In type-1 PFCM, we use the membership and typicality values which arise from the concept of fuzziness as opposed to the classical sets, where the membership can take values either 0 or 1. The membership values are computed using the degree of fuzziness, or the fuzzifier, m and similarly, typicality values are calculated using the parameter eta.

When we discuss about the fuzziness, we must also account for the fuzziness in the values of the fuzzifier m and the parameter η. This fuzziness leads us to extrapolate the Type-1 PFCM to Interval Type-2 PFCM and General Type-2 PFCM.

III. Proposed Algorithm

In case of type-2 fuzzy sets, we consider a fuzziness in the values of the fuzzifier m and the parameter η. This uncertainty in the fuzzifer and the parameter leads to an uncertainty in membership values and typicalities which further result in the formation of a footprint of uncertainty (FOU) of the membership function and typicality. The footprint of uncertainty (FOU) of a type-2 fuzzy set is a region with boundaries covering all the primary membership or typicality points of elements x. The more (less) area in the FOU the more (less) is the uncertainty. It is desirable to reduce the footprint of uncertainty without comprising on the information contained in it to make classification more accurate.The FOU of membership function gives the upper membership function(UMF) and the lower membership function(LMF)[19] and the FOU of typicality gives the upper typicality(UT) and the lower typicality(LT), denoted by, $\overline{u_x}$, $\underline{u_x}$, $\overline{t_x}$, $\underline{t_x}$ respectively.

We compute an interval for the possible membership function denoted by J_x, and the possible typicality values K_x, using (11) and (12).

The type-2 fuzzy sets are given by the equation as defined by Mendel in [18]:

$$\tilde{A} = \{((x, u), \mu_{\tilde{A}}(x, u)) \mid \forall x \in X, \forall u \in J_x \subseteq [\,0, 1\,]\} \tag{10}$$

$$J_x = [\,\underline{u_x}, \overline{u_x}\,] \tag{11}$$

$$K_x = [\,\underline{t_x}, \overline{t_x}\,] \tag{12}$$

In interval type-2 fuzzy sets, the interval J_x has a uniform distribution, that is, the secondary grade function, determining the distribution of the membership value in the interval J_x , is equal to one throughout the interval. In General type-2, however, this secondary grade function is not necessarily one and hence general type-2 provides one more degree of freedom over Interval Type-2, thus allowing the possibility of general type-2 PFCM outperforming interval type-2 PFCM.

In this paper, we propose two algorithms, Interval Type-2 PFCM and General Type-2 PFCM.

A. Interval Type-2 Possibilistic Fuzzy-C-Means

Extending an algorithm to type-2 increases the computational complexity by a considerable factor. However, taking the secondary grade function to be uniformly equal to one in the interval given by J_x reduces the complexity and provides an improvement over the algorithm applied to type-1 fuzzy sets. We represent interval type-2 fuzzy sets by the following equation:

$$\tilde{A} = \{((x,u), \mu_{\tilde{A}}(x,u)) \,|\, \forall x \in X, \forall u \in J_x \subseteq [\,0,1\,],\ \mu_{\tilde{A}}(x,u)) = 1\} \tag{13}$$

Uncertainty in the primary memberships of a type-2 fuzzy set, $\tilde{A}$, consists of a bounded region that we call the footprint of uncertainty (FOU). It is the union of all primary memberships[22], i.e.

$$FOU(\tilde{A}) = \bigcup_{x \in X} J_x \tag{14}$$

The shaded region in Fig. 1 is the FOU for membership function and Fig. 2 is the secondary grade membership function for interval type-2.

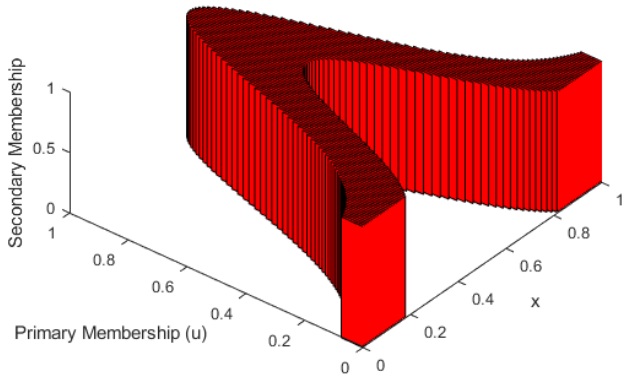

Fig. 1: IT2 footprint of uncertainty

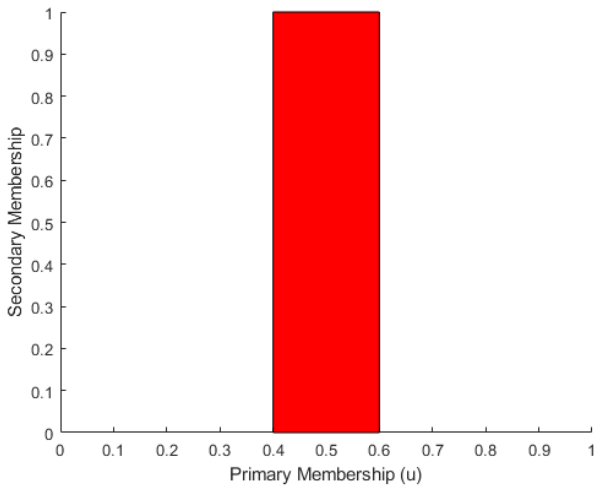

Fig. 2: IT2 secondary membership function

In interval type-2 PFCM (IT2-PFCM) we consider an interval for both the fuzzifier m and the parameter η and hence, for the membership and typicality values. We thus have a FOU for both. To account for the fuzziness in m, we consider a range for the possible values of m as $[m_1, m_2]$, and to account for the fuzziness in η, we consider a range for the possible values of η as $[\eta_1, \eta_2]$.

For i=1,2...c and k= 1,2...n, the FOU of membership function gives the upper membership function(UMF) and the lower membership function(LMF) which is computed using:

$$\overline{u_{ik}} = \begin{cases} \dfrac{1}{\sum_{j=1}^{c} (\frac{d_{ik}}{d_{jk}})^{\frac{2}{(m_1-1)}}} & if\ \dfrac{1}{\sum_{j=1}^{c} (\frac{d_{ik}}{d_{jk}})} < \frac{1}{c} \\ \dfrac{1}{\sum_{j=1}^{c} (\frac{d_{ik}}{d_{jk}})^{\frac{2}{(m_2-1)}}} & otherwise \end{cases} \tag{15}$$

$$\underline{u_{ik}} = \begin{cases} \dfrac{1}{\sum_{j=1}^{c} (\frac{d_{ik}}{d_{jk}})^{\frac{2}{(m_1-1)}}} & if\ \dfrac{1}{\sum_{j=1}^{c} (\frac{d_{ik}}{d_{jk}})} \geq \frac{1}{c} \\ \dfrac{1}{\sum_{j=1}^{c} (\frac{d_{ik}}{d_{jk}})^{\frac{2}{(m_2-1)}}} & otherwise \end{cases} \tag{16}$$

where,

$$d_{ik} = \|x_k - v_i\| \tag{17}$$

The FOU of the typicality gives the upper typicality(UT) and the lower typicality(LT) which is computed using:

$$\overline{t_{ik}} = \begin{cases} \dfrac{1}{1+(\frac{bd_{ik}^2}{\gamma_i})^{\frac{2}{\eta_1-1}}} & if\ \dfrac{1}{1+(\frac{bd_{ik}^2}{\gamma_i})^{\frac{2}{\eta_1-1}}} > \dfrac{1}{1+(\frac{bd_{ik}^2}{\gamma_i})^{\frac{2}{\eta_2-1}}} \\ \dfrac{1}{1+(\frac{bd_{ik}^2}{\gamma_i})^{\frac{2}{\eta_2-1}}} & otherwise \end{cases} \tag{18}$$

$$\underline{t_{ik}} = \begin{cases} \frac{1}{1+(\frac{bd_{ik}^2}{\gamma_i})^{\frac{2}{\eta_1-1}}} & if \ \frac{1}{1+(\frac{bd_{ik}^2}{\gamma_i})^{\frac{2}{\eta_1-1}}} \leq \frac{1}{1+(\frac{bd_{ik}^2}{\gamma_i})^{\frac{2}{\eta_2-1}}} \\ \frac{1}{1+(\frac{bd_{ik}^2}{\gamma_i})^{\frac{2}{\eta_2-1}}} & otherwise \end{cases} \tag{19}$$

where, $\gamma_i$is a constant defined as:

$$\gamma_i = K \frac{\sum_{k=1}^{n} u_{ik}^{'} d_{ik}^{'2}}{\sum_{k=1}^{n} u_{ik}^{'}} \tag{20}$$

where, $u_{ik}^{'}$ and $d_{ik}^{'2}$ are the membership values and distances between the pattern x_k and the cluster center v_i respectively, as computed from FCM clustering algorithm. In type-1 PFCM, we get crisp set of cluster centers denoted by v=$\{$ v_1, v_2...v_c $\}$, where, c gives the number of clusters. Since here we are using interval type-2 PFCM, we obtain an interval of the possible cluster centers given by v_R=$\{$ v_{1R}, v_{2R}...v_{mR} $\}$ and v_L=$\{$ v_{1L}, v_{2L}...v_{mL} $\}$, where v_R gives the rightmost boundary of the cluster center for each of the c clusters and v_L gives the leftmost boundary of the cluster center for each of the c clusters. We represent this interval by:

$$v_{\tilde{X}} = [\, v_L, v_R \,] \tag{21}$$

We perform type-reduction using EIASC algorithm [23] to obtain the above v_L and v_R from the initially set UMF and LMF and compute the crisp cluster center using the defuzzification equation:

$$v = \frac{v_L + v_R}{2} \tag{22}$$

The crisp cluster center obtained in the equation above is used to compute the membership and typicality values from (15),(16),(18) and (19). This process repeats iteratively until the optimal constant solution for the cluster centers is obtained. Once the cluster centroids are computed, final clustering is done by employing hard-partitioning in the following manner:

$$If \ d_{ki} < d_{kj}, \ for \ j = 1, 2c \ and \ i \neq j \ and \ k = 1, 2n, \quad then, \ x_k \ is \ assigned \ to \ the \ cluster \ i. \tag{23}$$

We now give a step-by-step description of the proposed interval type-2 PFCM followed by a flowchart of the same:

Step 1. Set the values of fuzzifiers m_1 and m_2; parameter $\eta_1$and η_2; constants a and b. Set the initial cluster centers as v'=$\{$ v'_1, v'_2...v'_m $\}$.

Step 2. Calculate the distances d_{ik} using equation(17). The membership values $\overline{u}_{ik}$, $\underline{u}_{ik}$ using equations (15) and (16); γ_i using equations (20); the typicality values $\overline{t}_{ik}$, $\underline{t}_{ik}$ using equations (18) and (19); and set m and η to arbitrary values. Compute the centroids $v'_{i,RU}$, $v'_{i,RT}$, $v'_{i,LU}$ and $v'_{i,LT}$ using the values u_{ik} and t_{ik}, where

$$u_{ik} = \frac{\overline{u}_{ik} + \underline{u}_{ik}}{2} \tag{24}$$

$$t_{ik} = \frac{\overline{t}_{ik} + \underline{t}_{ik}}{2} \tag{25}$$

$$v'_{i,RU} = v'_{i,LU} = \frac{\sum_{k=1}^{n} (u_{ik})^m X_k}{\sum_{k=1}^{n} (u_{ik})^m} \tag{26}$$

$$v'_{i,RT} = v'_{i,LT} = \frac{\sum_{k=1}^{n} (t_{ik})^m X_k}{\sum_{k=1}^{n} (t_{ik})^m} \tag{27}$$

Step 3. Apply EIASC algorithm to calculate $v'_{i,L}$ and $v'_{i,R}$ separately and compute the new cluster centers by the equation:

$$v''_i = \frac{v'_{i,R} + v'_{i,L}}{2} \tag{28}$$

where, $v'_{i,L}$ and $v'_{i,R}$ are computed using:

$$v'_{i,L} = \frac{\sum_{k=1}^{n} (a u_i(x_k)^m + b t_i(x_k)^\eta) x_k}{\sum_{k=1}^{n} (a u_i(x_k)^m + b t_i(x_k)^\eta)} \tag{29}$$

$$v'_{i,R} = \frac{\sum_{k=1}^{n} (a u_i(x_k)^m + b t_i(x_k)^\eta) x_k}{\sum_{k=1}^{n} (a u_i(x_k)^m + b t_i(x_k)^\eta)} \tag{30}$$

and hence, we get the new set of cluster centroids given by v''=$\{$ v''_1, v''_2....v''_m $\}$

Step 4. Compare the cluster centroids v' and v''. If each cluster centroid satisfies the condition, $\parallel v_i' - v_i'' \parallel < \epsilon$, where ϵ is the error threshold value, we proceed to Step 5., else update v' as given below and continue with step 2 until the cluster centroids converge.

$$v' = v'' \tag{31}$$

Step 5. Set the final center centroids as v and perform hard partition according to the equation (23).

$$v = v'' \tag{32}$$

In IT2-PFCM we employ the use of EIASC algorithm for type-reduction purposes, which ultimately returns the interval of the cluster centroids for every cluster. The EIASC algorithm is demonstrated below.

TABLE I: EIASC Pseudocode

Step	EIASC for c_l	EIASC for c_r
1:	Initialize	Initialize
	$a = \sum_{i=1}^{N} x_i \underline{\mu}_{\tilde{A}}(x_i)$	$a = \sum_{i=1}^{N} x_i \bar{\mu}_{\tilde{A}}(x_i)$
	$b = \sum_{i=1}^{N} \underline{\mu}_{\tilde{A}}(x_i)$	$b = \sum_{i=1}^{N} \bar{\mu}_{\tilde{A}}(x_i)$
	L=0	R=N
2:	Compute	Compute
	L=L+1	$a = a + x_R[\bar{\mu}_{\tilde{A}}(x_R) - \underline{\mu}_{\tilde{A}}(x_R)]$
	$a = a + x_L[\bar{\mu}_{\tilde{A}}(x_L) - \underline{\mu}_{\tilde{A}}(x_L)]$	$b = b + [\bar{\mu}_{\tilde{A}}(x_R) - \underline{\mu}_{\tilde{A}}(x_R)]$
	$b = b + [\bar{\mu}_{\tilde{A}}(x_L) - \underline{\mu}_{\tilde{A}}(x_L)]$	$c_r = a/b$
	$c_l = a/b$	R=R-1
3:	if $c_l \leq x_{L+1}$, break	if $c_r \geq x_R$, break
	else go to Step (b).	else repeat Step (b).

We further demonstrate our algorithm with IT2-PFCM flowchart in Figure 3.

B. General Type-2 Possibilistic Fuzzy-C-Means

Type-2 fuzzy sets are incorporated to account for the uncertainty in the values of the fuzzifier m and the parameter η. In interval type-2, we consider an interval for both the m and η with uniform distribution of one throughout the interval. This constrains the distribution in the interval thereby effectively resulting in a blurred type-1 fuzzy set. In general type-2, the distribution of m and η in the interval J_x and K_x respectively, is given by a secondary grade membership function, $\mu_{\tilde{A}}(x,u)$ which thus results in general type-2 fuzzy sets having more degree of freedoms as compared to interval type-2 fuzzy sets.

Due to the availability of another degree of freedom in general type-2 fuzzy sets, we now apply PFCM to general type-2 (GT2-PFCM) which is shown to outperform IT2-PFCM.

A general type-2 fuzzy set is represented as in the equation (10). The general type-2 FOU and secondary membership function are shown in Figure 4 and 5 respectively.

The FOU of membership values of general type-2 fuzzy set is bounded by UMF and LMF which are denoted by $\overline{u_{ik}}$ and $\underline{u_{ik}}$; and the FOU of typicalities are bounded by UT and LT denoted by $\overline{t_{ik}}$ and $\underline{t_{ik}}$ respectively. These values define J_x and K_x and hence account for fuzziness in the values of m and η. In IT2-PFCM took an average of $\overline{u_{ik}}$ and $\underline{u_{ik}}$ to compute the membership function u_{ik}; and the average of $\overline{t_{ik}}$ and $\underline{t_{ik}}$ to compute the typicality t_{ik} as per the equations (25) and (26). However, this was possible because in interval type-2 the secondary grade function is uniformly one throughout the fuzzy interval. In case of general type-2, the secondary grade is not uniform and hence there are unequal weights of values lying in the interval J_x and K_x.

To apply PFCM to general type-2 fuzzy sets, we use the α-planes representation of general type-2 fuzzy sets as suggested by Linda and Manic for GT2-FCM in [21]. An α-plane $\tilde{A_\alpha}$ of a GT2 fuzzy set $\tilde{A}$ can be defined as the union of all primary memberships of $\tilde{A}$ with secondary grades greater than or equal to α.

$$\tilde{A_\alpha} = \int_{\forall x \in A} \int_{\forall \mu \in J_x} \{(x,u) | \mu_{\tilde{A}} \geq \alpha\} \tag{33}$$

The α-cut of secondary membership function can be denoted as $S_{\tilde{A}}(x|\alpha)$ and its interval is represented as:

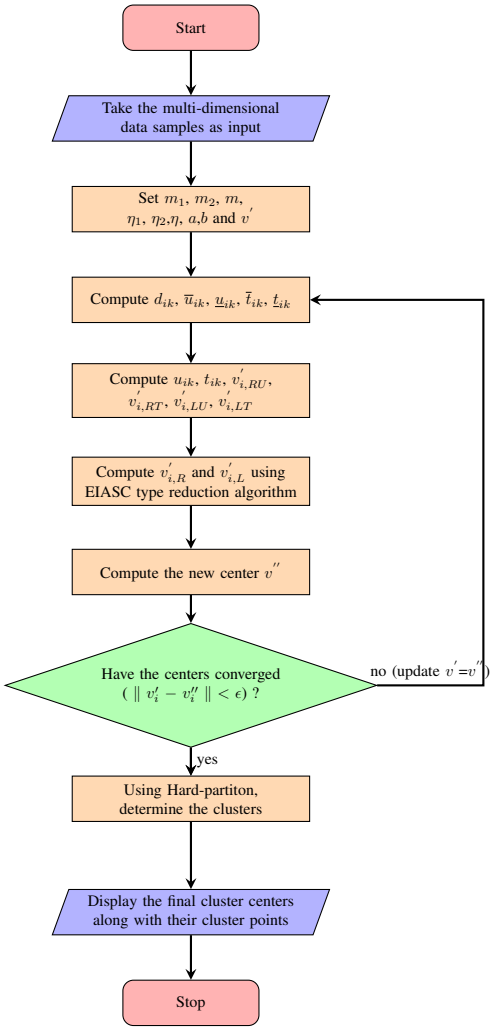

Fig. 3: IT2 PFCM algorithm flowchart

$$S_{\tilde{A}}(x|\alpha) = [\, s^{L}_{\tilde{A}}(x|\alpha), s^{R}_{\tilde{A}}(x|\alpha)\,] \tag{34}$$

Thus, we can repesent an α-plane as a composition of α-cuts of all secondary membership functions.

$$\tilde{A_\alpha} = \int_{\forall x \in A} S_{\tilde{A}}(x|\alpha) \tag{35}$$

By raising the α-plane $\tilde{A_\alpha}$ to the level of α, a special IT2 fuzzy set is created. This set was named α-level T2 fuzzy set $R_{\tilde{A_\alpha}}(x,u)$ in [20] and [24] and was denoted as:

$$R_{\tilde{A_\alpha}}(x,u) = \alpha/\tilde{A_\alpha} \forall x \ \in A, \forall \mu \ \in J_x \tag{36}$$

The GT2 fuzzy set $\tilde{A}$ can be constructed from the composition of all the α-level T2 fuzzy sets:

$$\tilde{A} = \bigcup_{\alpha \in [0,1]} \alpha/\tilde{A_\alpha} \tag{37}$$

In T2 PFCM, we need to find the uncertainty involved with the fuzzifier m and the parameter η. For IT2-PFCM, we define the intervals $[m_1\ ,\ m_2]$ and $[\eta_1\ ,\ \eta_2]$, which have a uniform distribution of uncertainty about the appropriate value of the fuzzifier m and parameter η.In the case of GT2 PFCM, the concept of linguistic fuzzifier is used, which is denoted by a type-1 fuzzy set(e.g. small orhigh), M[21].Since PFCM another parameter η, we extend this theory to η as well by taking linguistic paramter as H. Two examples of depicting the linguistic notion of the appropriate fuzzifier(parameter) value for the GT2 PFCM algorithm is shown using three linguistic terms in Fig. 6. We represent the linguistic fuzzifier(paramter), M(H), with the help of its α-cuts as follows:

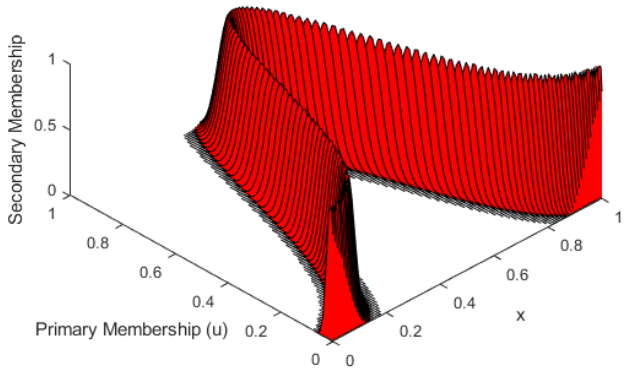

Fig. 4: GT2 footprint of uncertainty

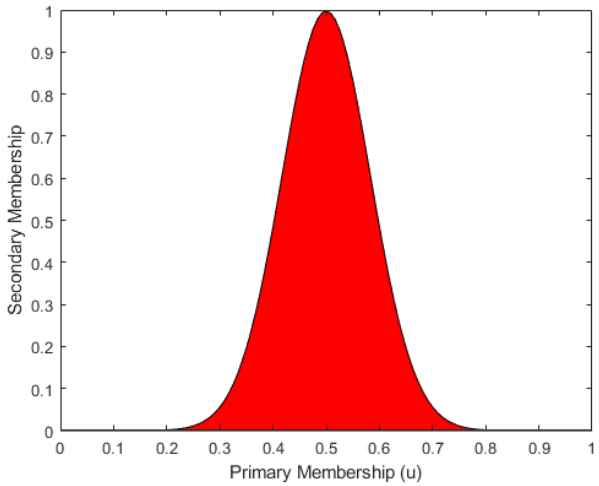

Fig. 5: GT2 secondary membership function

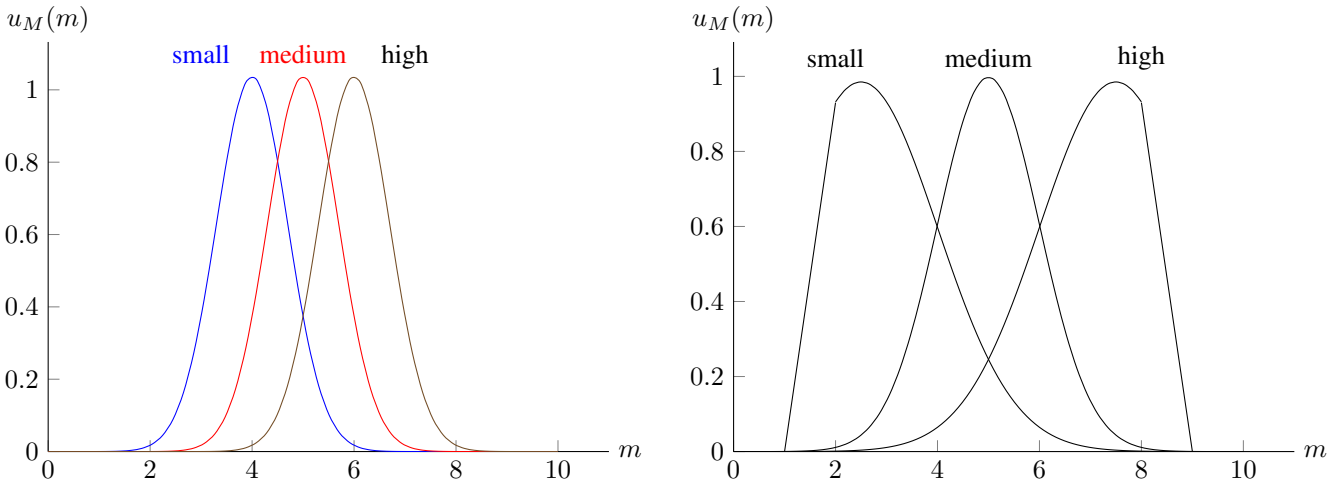

Fig. 6: Two representations of the linguistic fuzzifier *M*

$$M = \bigcup_{\alpha \in [0,1]} \alpha / S_M(\alpha) \tag{38}$$

and,

$$H = \bigcup_{\alpha \in [0,1]} \alpha / S_H(\alpha) \tag{39}$$

where,

$$S_M(x|\alpha) = [\, s_M^L(x|\alpha), s_M^R(x|\alpha) \,] \tag{40}$$

and,

$$S_H(x|\alpha) = [\, s_H^L(x|\alpha), s_H^R(x|\alpha) \,] \tag{41}$$

The linguistic fuzzifier, M, and the linguistic paramter, H, are used to construct the secondary membership funcions for our GT2 model. The GT2 fuzzy membership function and typicality for cluster v_i can be obtained as:

$$\tilde{u}_i = \sum_{x_k \in X} \tilde{u}_{ik} \tag{42}$$

and

$$\tilde{t}_i = \sum_{x_k \in X} \tilde{t}_{ik} \tag{43}$$

The secondary membership function $\tilde{u}_{ik}$ and secondary typicality $\tilde{t}_{ik}$ can be expressed with the help of α-cuts as follows:

$$\tilde{u}_{ik} = \bigcup_{\alpha \in [0,1]} \alpha / S_{\tilde{u}_i}(x_k/\alpha) = \bigcup_{\alpha \in [0,1]} \alpha / [\, s^L_{\tilde{u}_i}(x_k|\alpha), s^R_{\tilde{u}_i}(x_k|\alpha)\,] \tag{44}$$

and

$$\tilde{t}_{ik} = \bigcup_{\alpha \in [0,1]} \alpha / S_{\tilde{t}_i}(x_k/\alpha) = \bigcup_{\alpha \in [0,1]} \alpha / [\, s^L_{\tilde{t}_i}(x_k|\alpha), s^R_{\tilde{t}_i}(x_k|\alpha)\,] \tag{45}$$

Thus, we see that with this representation of the seconday membership and typicality function as linguistic fuzzifier, B, and linguistic parameter ,H, having α-planes at different levels, the secondary membership and typicality degrees can be calculated by a combination of IT2 fuzzy sets. The upper and lower boundaries of the secondary degrees for each α-plane in determined from B and H. Let the number of α-planes considered be p with α=α_1, α_2....α_p. The upper and lower boundaries for the secondary membership degree and typicality value is calculated as follows:

$$s^L_{\tilde{u}_i}(x_k|\alpha) = \begin{cases} \frac{1}{\sum_{l=1}^{c} (\frac{d_{ik}}{d_{lk}})^{(\frac{2}{s^L_M(\alpha)-1})}} & if \ \frac{1}{\sum_{l=1}^{c} (\frac{d_{ik}}{d_{lk}})^{(\frac{2}{s^L_M(\alpha)-1})}} \leq \frac{1}{\sum_{l=1}^{c} (\frac{d_{ik}}{d_{lk}})^{(\frac{2}{s^R_M(\alpha)-1})}} \\ \frac{1}{\sum_{l=1}^{c} (\frac{d_{ik}}{d_{lk}})^{(\frac{2}{s^R_M(\alpha)-1})}} & otherwise \end{cases} \tag{46}$$

$$s^R_{\tilde{u}_i}(x_k|\alpha) = \begin{cases} \frac{1}{\sum_{l=1}^{c} (\frac{d_{ik}}{d_{lk}})^{(\frac{2}{s^L_M(\alpha)-1})}} & if \ \frac{1}{\sum_{l=1}^{c} (\frac{d_{ik}}{d_{lk}})^{(\frac{2}{s^L_M(\alpha)-1})}} > \frac{1}{\sum_{l=1}^{c} (\frac{d_{ik}}{d_{lk}})^{(\frac{2}{s^R_M(\alpha)-1})}} \\ \frac{1}{\sum_{l=1}^{c} (\frac{d_{ik}}{d_{lk}})^{(\frac{2}{s^R_M(\alpha)-1})}} & otherwise \end{cases} \tag{47}$$

and,

$$s^L_{\tilde{t}_i}(x_k|\alpha) = \begin{cases} \frac{1}{1+(\frac{bd^2_{ik}}{\gamma_i})^{\frac{2}{s^L_H-1}}} & if \ \frac{1}{1+(\frac{bd^2_{ik}}{\gamma_i})^{\frac{2}{s^L_H-1}}} \leq \frac{1}{1+(\frac{bd^2_{ik}}{\gamma_i})^{\frac{2}{s^R_H-1}}} \\ \frac{1}{1+(\frac{bd^2_{ik}}{\gamma_i})^{\frac{2}{s^R_H-1}}} & otherwise \end{cases} \tag{48}$$

$$s^R_{\tilde{t}_i}(x_k|\alpha) = \begin{cases} \frac{1}{1+(\frac{bd^2_{ik}}{\gamma_i})^{\frac{2}{s^L_H-1}}} & if \ \frac{1}{1+(\frac{bd^2_{ik}}{\gamma_i})^{\frac{2}{s^L_H-1}}} > \frac{1}{1+(\frac{bd^2_{ik}}{\gamma_i})^{\frac{2}{s^R_H-1}}} \\ \frac{1}{1+(\frac{bd^2_{ik}}{\gamma_i})^{\frac{2}{s^R_H-1}}} & otherwise \end{cases} \tag{49}$$

where, i=1,2...c and k=1,2...n and γ_i is as computed in equation (20).

In IT2 PFCM, we computed u_{ik} and t_{ik} using equations (25) and (26), in case of GT-2, we compute u_{ik} and t_{ik} as follows:

$$u_{ik} = \frac{\sum_{l=1}^{p} \alpha_l (s^L_{\tilde{u}_i}(x_k|\alpha) + s^R_{\tilde{u}_i}(x_k|\alpha))}{2\sum_{l=1}^{p} \alpha_l} \tag{50}$$

$$t_{ik} = \frac{\sum_{l=1}^{p} \alpha_l (s^L_{\tilde{t}_i}(x_k|\alpha) + s^R_{\tilde{t}_i}(x_k|\alpha))}{2\sum_{l=1}^{p} \alpha_l} \tag{51}$$

The resulting u_{ik} and t_{ik} are used in the GT2-PFCM algorithm to determine the cluster prototypes and hence the clusters. We now provide a step-by-step description of our proposed algorithm followed by a flowchart of the same:

Step 1. Set the values of fuzzifiers m, m_1 and m_2; parameter η, $\eta_1$and η_2; constants a and b. Set the initial cluster centers as v'=$\{\ v'_1, v'_2...v'_c\ \}$.

Step 2. Calculate the distances d_{ik} using equation(17).Consider a representation of the linguistic fuzzifier M and parameter H from Fig. 6, and consider p α-cuts, with α-levels as α_1, α_2...α_p.For the yth α-cut, compute an interval of the fuzzifier given by $[m_{1y}, m_{2y}]$ and of the parameter given by $[\eta_{iy},\eta_{2y}]$. For every $y \in [1, p]$, compute $\overline{u}_{iyk}$ and $\underline{u}_{iyk}$, $\overline{t}_{iyk}$ and $\overline{t}_{iyk}$ using the following equations and hence compute u_{iyk} and t_{iyk}.

$$\overline{u}_{iyk} = \begin{cases} \frac{1}{\sum_{j=1}^{c}(\frac{d_{ik}}{d_{jk}})^{\frac{2}{(m_{1y}-1)}}} & if \ \frac{1}{\sum_{j=1}^{c}(\frac{d_{ik}}{d_{jk}})} < \frac{1}{c} \\ \frac{1}{\sum_{j=1}^{c}(\frac{d_{ik}}{d_{jk}})^{\frac{2}{(m_{2y}-1)}}} & otherwise \end{cases} \tag{52}$$

$$\underline{u}_{iyk} = \begin{cases} \frac{1}{\sum_{j=1}^{c}(\frac{d_{ik}}{d_{jk}})^{\frac{2}{(m_{1y}-1)}}} & if \ \frac{1}{\sum_{j=1}^{c}(\frac{d_{ik}}{d_{jk}})} \geq \frac{1}{c} \\ \frac{1}{\sum_{j=1}^{c}(\frac{d_{ik}}{d_{jk}})^{\frac{2}{(m_{2y}-1)}}} & otherwise \end{cases} \tag{53}$$

$$\bar{t}_{iyk} = \begin{cases} \frac{1}{1+(\frac{bd_{ik}^2}{\gamma_i})^{\frac{2}{\eta_{1y}-1}}} & if \ \frac{1}{1+(\frac{bd_{ik}^2}{\gamma_i})^{\frac{2}{\eta_{1y}-1}}} > \frac{1}{1+(\frac{bd_{ik}^2}{\gamma_i})^{\frac{2}{\eta_{2y}-1}}} \\ \frac{1}{1+(\frac{bd_{ik}^2}{\gamma_i})^{\frac{2}{\eta_{2y}-1}}} & otherwise \end{cases} \tag{54}$$

$$\underline{t}_{iyk} = \begin{cases} \frac{1}{1+(\frac{bd_{ik}^2}{\gamma_i})^{\frac{2}{\eta_{1y}-1}}} & if \ \frac{1}{1+(\frac{bd_{ik}^2}{\gamma_{\ i}})^{\frac{2}{\eta_{1y}-1}}} \leq \frac{1}{1+(\frac{bd_{ik}^2}{\gamma_i})^{\frac{2}{\eta_{2y}-1}}} \\ \frac{1}{1+(\frac{bd_{ik}^2}{\gamma_i})^{\frac{2}{\eta_{2y}-1}}} & otherwise \end{cases} \tag{55}$$

where, γ_i is computed using equation (20), and,

$$u_{iyk} = \frac{\underline{u}_{iyk} + \overline{u}_{iyk}}{2} \tag{56}$$

$$t_{iyk} = \frac{\underline{t}_{iyk} + \bar{t}_{iyk}}{2} \tag{57}$$

Step 3. Using the u_{iyk} and t_{iyk}, compute the centroids $v'_{iy,RU}$, $v'_{iy,RT}$, $v'_{iy,LU}$ and $v'_{iy,LT}$, where,

$$v'_{iy,RU} = v'_{i,LU} = \frac{\sum_{k=1}^{n}(u_{iyk})^m X_k}{\sum_{k=1}^{n}(u_{iyk})^m} \tag{58}$$

$$v'_{iy,RT} = v'_{i,LT} = \frac{\sum_{k=1}^{n}(t_{iyk})^m X_k}{\sum_{k=1}^{n}(t_{iyk})^m} \tag{59}$$

Step 4. For every $y \in [1, p]$, apply EIASC algorithm to calculate $v'_{iy,L}$ and $v'_{iy,R}$ separately and compute the new cluster centers by the equation:

$$v''_i y = \frac{v'_{iy,R} + v'_{iy,L}}{2} \tag{60}$$

where, $v'_{iy,L}$ and $v'_{iy,R}$ are computed using:

$$v'_{iy,L} = \frac{\sum_{k=1}^{n}(au_{iy}(x_k)^m + bt_{iy}(x_k)^\eta)x_k}{\sum_{k=1}^{n}(au_{iy}(x_k)^m + bt_{iy}(x_k)^\eta)} \tag{61}$$

$$v'_{iy,R} = \frac{\sum_{k=1}^{n}(au_{iy}(x_k)^m + bt_{iy}(x_k)^\eta)x_k}{\sum_{k=1}^{n}(au_{iy}(x_k)^m + bt_{iy}(x_k)^\eta)} \tag{62}$$

and hence, we get the new set of cluster centroids given by v''={ v''_1, v''_2....v''_c }, where,

$$v''_i = \frac{\sum_{y=1}^{p}\alpha_y v''_{iy}}{2\sum_{y=1}^{p}\alpha_y} \tag{63}$$

where, i=1,2...c.

Step 5. Compare the cluster centroids v' and v''. If each cluster centroid satisfies the condition, $\parallel v'_i - v''_i \parallel < \epsilon$, where ϵ is the error threshold value, we proceed to Step 6., else update v' as given below and continue with step 2 until the cluster centroids converge.

$$v' = v'' \tag{64}$$

Step 6. Set the final center centroids as v and perform hard partition according to the equation (23) where, u_{ik} and t_{ik} are computed using equations (50) and (51).

$$v = v'' \tag{65}$$

We now demonstrate our proposed algorithm by a flowchart as shown in Figure 8.

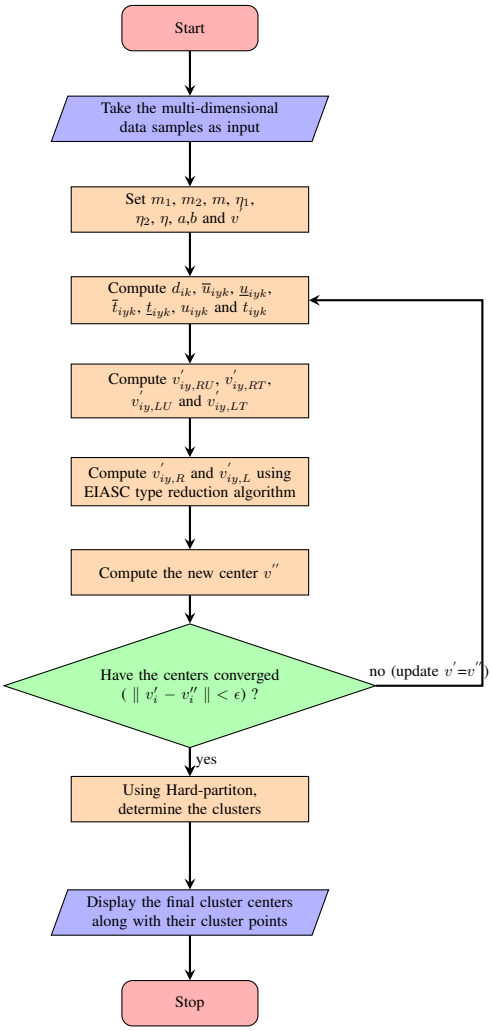

Fig. 7: GT2 PFCM algorithm flowchart

IV. Experimental Results

To check the validity and efficiency of our proposed algortihms, we test our algorithm on various datasets with diffeent dimensionality. We compare the recognition rate of PFCM, IT2-PFCM amd GT2-PFCM and estimate the accuracy and robustness of our proposed algorithms against type-1 PFCM by varying different parameters, like the user-defined constants a and b, the fuzzifier m and the parameter η. We test the above algorithms on Iris dataset and Wisconsin breast cancer dataset. We vary the constants a and b in the interval [1,30] in steps of 3, and m and eta in the interval [1,15] in unit steps. In case of IT2-PFCM and GT2-PFCM, we vary m_1 (η_1) in the above range and choose m_2 (η_2) such that the resulting accuracy achieved is the most optimum for the given m_1 ((η_1)). The linguistic fuzzifier and parameter, M and H respectively, used for secondary membership function of GT2-PFCM is *'medium'* from Fig. 6. For representation of GT2 fuzzy sets, we use five α-cuts.

A. Iris Dataset

Iris dataset[25] has 4 attributes, 150 datapoints and 3 classes(each having 50 samples). We apply PFCM, IT2-PFCM and GT2-PFCM to iris dataset and compare the resulting accuracies. For PFCM, we get an accuracy of 91.33% with the corresponding values of m and eta equal to 2 and 3 respectively. However, for IT2 and GT2-PFCM, we get an increased recognition rate of 94.67% and 95.33% respectively, with the m_1, m_2, η_1 and η_2 taking the values 2.9, 3, 2 and 3 respectively. For obtaining

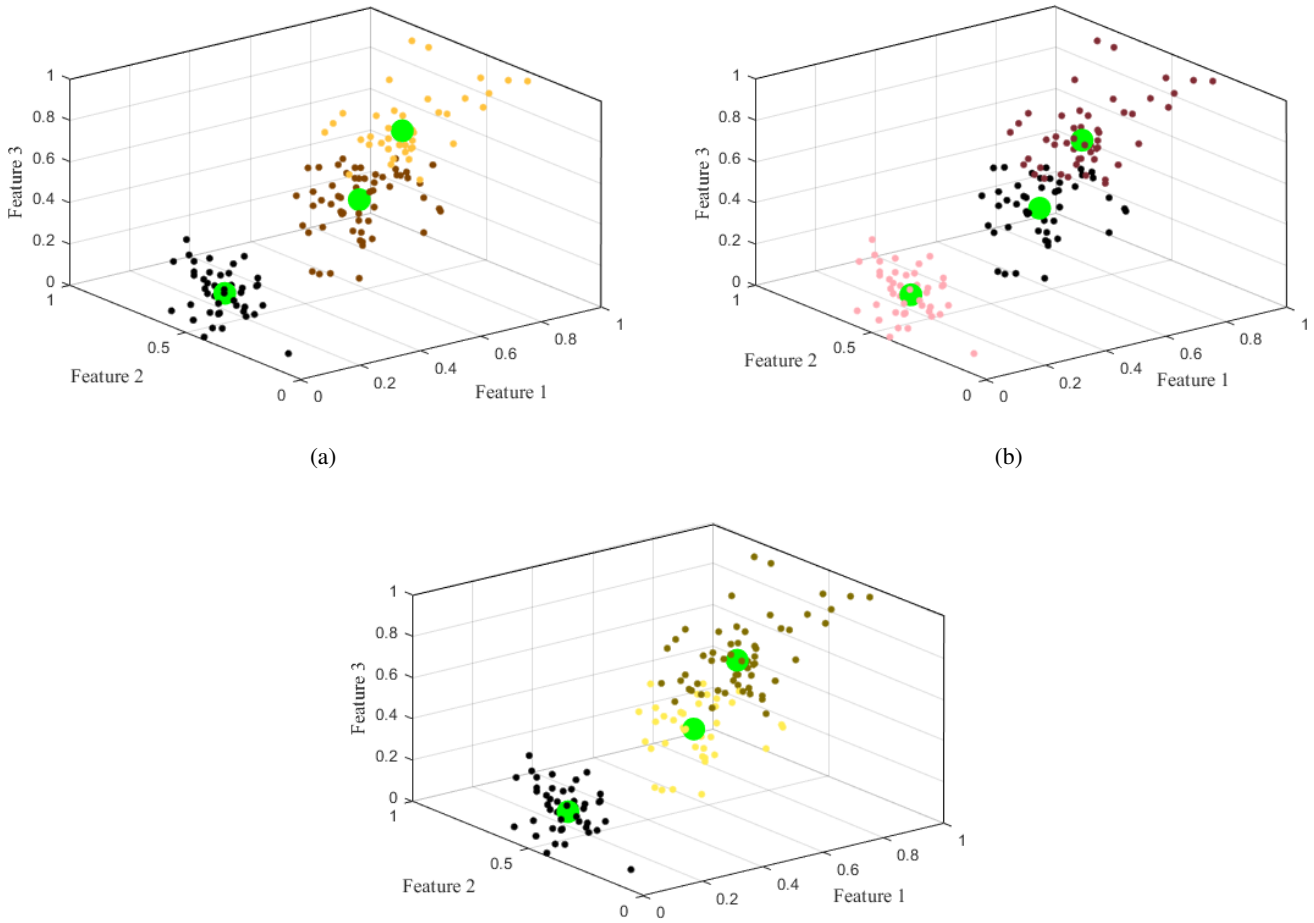

Fig. 8: Clusters formation of Iris dataset: (a) Type 1 PFCM, (b) Interval Type 2 PFCM and (c) General Type 2 PFCM

these results, we use an error threshold value of 0.0001, denoted by ϵ. We show the cluster plots for the results of PFCM, IT2-PFCM and GT2-PFCM in Fig.8.

Table II summarizes our results with the values of various parameters used to obtain them and Table III shows the confusion matrix of the results of each of the three algorithms.

TABLE II: Maximum recognition rate obtained for , Type 1 PFCM, IT2 and GT2 PFCM for Iris dataset

Algorithm	Constant (a)	Constant (b)	Fuzzifier (m)	Parameter (η)	Recognition rate(%)
T1 PFCM	1	5	2	3	91.33
IT2 PFCM	1	5	m_1=2.9 m_2=3	η_1=2 η_2=3	94.67
GT2 PFCM	1	5	m_1=2.9 m_2=3	η_1=2 η_2=3	95.33

B. Wisconsin Breast Cancer Dataset

Wisconsin Breast Cancer dataset[25] has 8 attributes, 699 datapoints and 2 classes(classes being defined as Malignant or Benign). We apply PFCM, IT2-PFCM and GT2-PFCM to this dataset and compare the resulting accuracies. For PFCM, we get an accuracy of 95.71% with the corresponding values of m and eta equal to 2 and 3 respectively. However, for IT2 and GT2-PFCM, we get an increased recognition rate of 96.42% and 96.57% respectively with the m_1, m_2, η_1 and η_2 taking the

TABLE III: Confusion matrices for the best results in Type 1 PFCM, Interval and General type 2 PFCM algorithms for Iris dataset

Algorithm	True Class \ Recognised Class	1	2	3
T1 PFCM	1	50	0	0
	2	0	46	4
	3	0	9	41
IT2 PFCM	1	50	0	0
	2	1	44	5
	3	0	2	48
GT2 PFCM	1	50	0	0
	2	0	48	2
	3	0	5	45

values 2, 3, 2 and 3 respectively. For obtaining these results, we use an error threshold value of 0.0001, denoted by ϵ. We show the cluster plots for the results of PFCM, IT2-PFCM and GT2-PFCM in Fig.9.

We now summarize our results for the best accuracy rates in Table IV with various parameters used in the algorithm.

TABLE IV: Maximum recognition rate obtained for , Type 1 PFCM, IT2 and GT2 PFCM for Wisconsin Breast Cancer dataset

Algorithm	Constant (a)	Constant (b)	Fuzzifier (m)	Parameter (η)	Recognition rate(%)
T1 PFCM	1	5	2	3	95.71
IT2 PFCM	1	5	m_1=2 m_2=3	η_1=2 η_2=3	96.42
GT2 PFCM	1	5	m_1=2 m_2=3	η_1=2 η_2=3	96.57

Table V shows the confusion matrix of the results of each of the three algorithms.

TABLE V: Confusion matrices for the best results in Type 1 PFCM, Interval and General type 2 PFCM algorithms for Wisconsin Breast Cancer dataset

Algorithm	True Class \ Recognised Class	1	2
T1 PFCM	1	444	14
	2	16	225
IT2 PFCM	1	442	16
	2	9	232
GT2 PFCM	1	438	20
	2	4	237

We now observe the recognition rate and robustness as resulted by our proposed algorithm as compared to Type-1 PFCM while we vary the user-defined constants a, b and the fuzzifier m and parameter η. In type-1, fuzzifier and parameter stand for m and η respectively, however, in IT2-PFCM and GT2-PFCM, fuzzifier imples m_1 and parameter implies η_1. We vary $m_1(\eta_1)$ and use $m_2(\eta_2)$ for which recognition rate is maximum.

From Fig. 10 we observe that for Type-1 PFCM, the increase in the value of b increases the training set error (slightly though) because it reduces the importance of the membership, and hence the typicality values have a greater influence on the clustering results. The partition matrix (U) is the sole basis on which hard partitioning is done, and since the membership values are less accurate it implies that hard-partitioning is also inaccurate. In case on IT2-PFCM and GT2-PFCM, increase in the value of b intially decreases the error rate but on further increase, the error rate increases and remains constant thereafter.

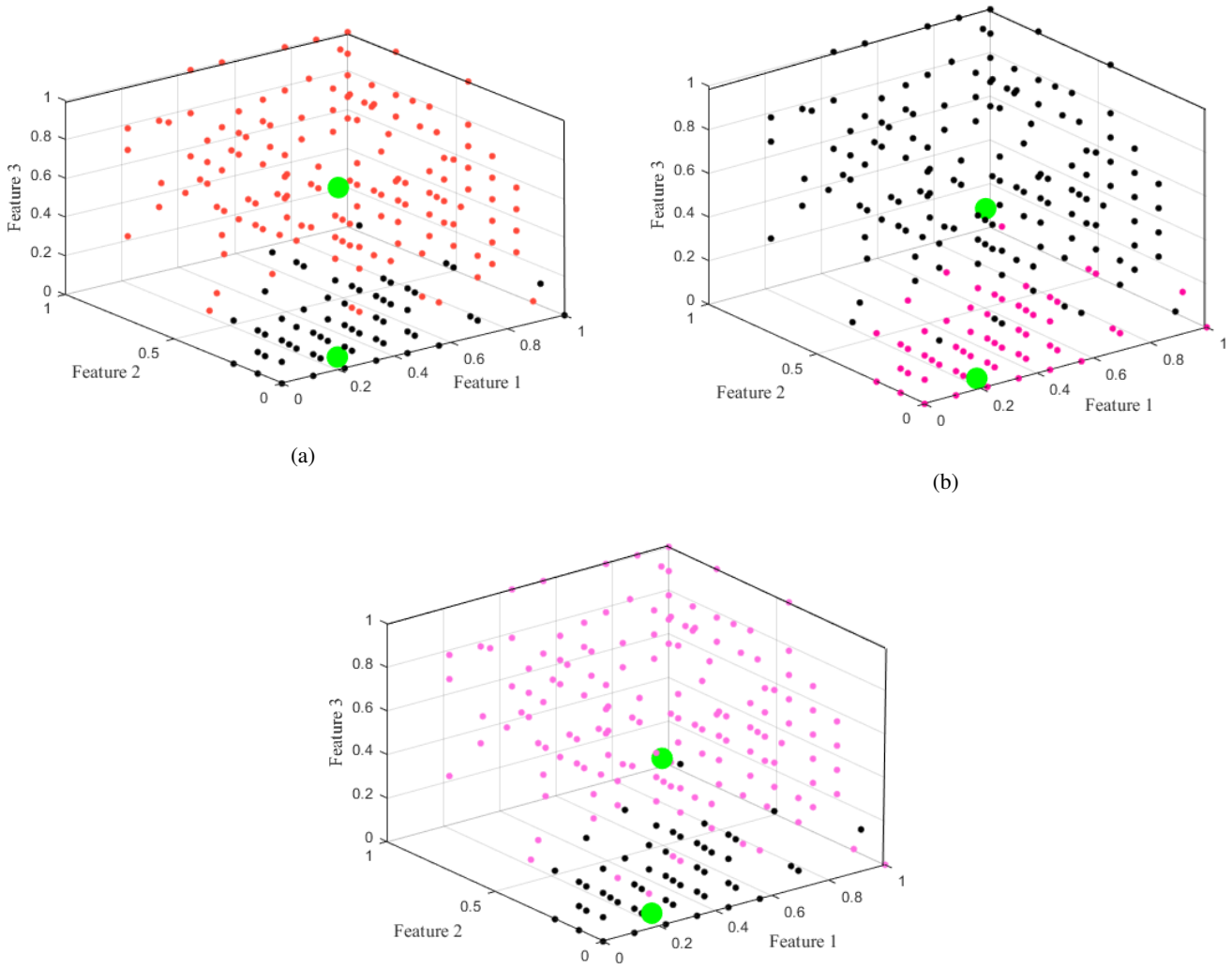

Fig. 9: Clusters formation of Wisconsin Breast Cancer dataset: (a) Type 1 PFCM, (b) Interval Type 2 PFCM and (c) General Type 2 PFCM

C. Wine Dataset

We now compare the results of Type-1 PFCM with our proposed algorithms on Wine dataset[24]. Wine dataset contains 13 attributes, 178 samples and 3 classes. As shown in Table VI, type-1 PFCM shows an accuracy of 70.79%, IT2-PFCM and GT2-PFCM show a considerable increase in accuracy with recognition rate being 72.48% and 74.16% respectively.

TABLE VI: Maximum recognition rate obtained for , Type 1 PFCM, IT2 and GT2 PFCM for Wine dataset

Algorithm	Constant (a)	Constant (b)	Fuzzifier (m)	Parameter (η)	Recognition rate(%)
T1 PFCM	1	5	2	3	70.79
IT2 PFCM	1	5	m_1=1.2 m_2=5	η_1=2 η_2=3	72.48
GT2 PFCM	1	5	m_1=1.2 m_2=5	η_1=2 η_2=3	74.16

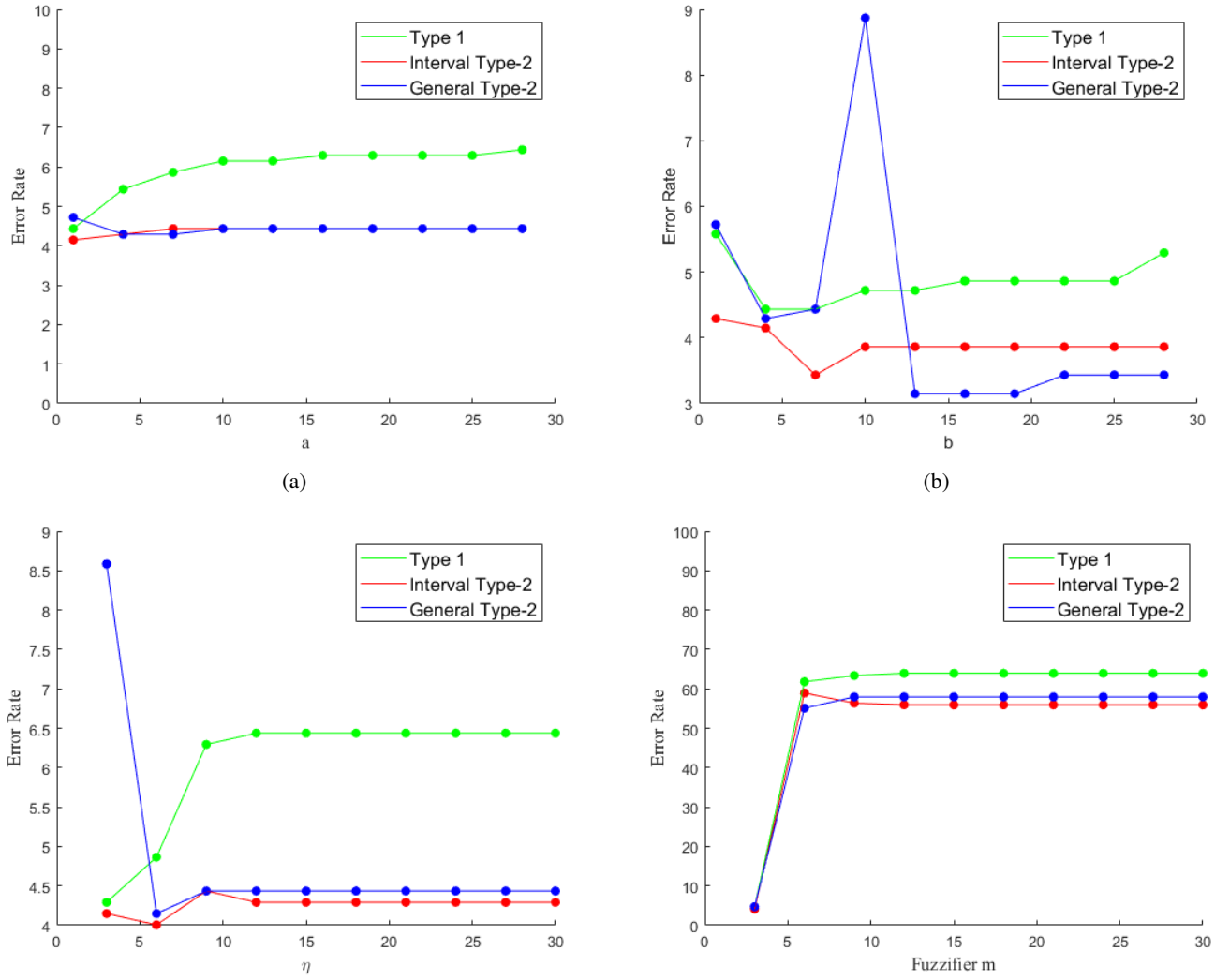

Fig. 10: Error plot for T1 PFCM, interval and general type-2 PFCM clustering results against (a) a, (b) b, (c) η and (d) m.

TABLE VII: Confusion matrices for the best results in Type 1 PFCM, Interval and General type 2 PFCM algorithms for Wine dataset

Algorithm	Recognised Class / True Class	1	2	3
T1 PFCM	1	46	0	13
	2	1	50	20
	3	0	18	30
IT2 PFCM	1	48	0	11
	2	2	49	20
	3	0	16	32
GT2 PFCM	1	55	0	4
	2	4	44	23
	3	6	9	33

D. Image Segmentation

Finally, to demonstrate our algorithms, we choose four 200×200 natural scene images. Each image has three sections: road, forest and sky. The feature images that we use for our segmentation are median filtered intensity, entropy and Gaussian blur.

We randomly choose 100 pixels from each region of an image and and give their respective feature values as the data input to the algorithms. Hence we have a total of 300 sample pixels for each image. Once we have trained our data and the clusters have been formed, we assign the rest of the points using the concept of K- nearest neighbours. For each pixel in the image we find the K nearest sample pixels based on the feature images and assign the pixel to that cluster to which maximum of the K nearest pixels belong. This is repeated for all the remaining pixels. In order to find the recognition rate, we compare our results with the mask image for each scene.

The feature images of Scene 1 are shown in Fig. 11(d)-(f). The rest have been ignored due to repetitiveness. The segmented images obtained for Scene 1 by using the various PFCM algorithms have been depicted in Figure 11(g)-(i). A scatter plot of the selected 300 pixels for training the data has been shown in Fig. 11(c), 12(c) and 13(c) for scene 1, 2 and 3 respectively.The road, forest and sky have been denoted by the symbols $\square$, $\circ$ and $\times$ respectively. It can be observed that our proposed IT2 and GT2 algorithms show an improvement in accuracy. The confusion matrices and recognition rate has been tabulated in Table VIII-XII.

TABLE VIII: Maximum Recognition Rates for T1-PFCM, IT2-PFCM and GT2-PFCM for Scene-1, Scene-2 and Scene-3

Algorithm	Image	Recognition Rate
T1 PFCM	S1	89.90
	S2	87.83
	S3	95.87
IT2 PFCM	S1	90.73
	S2	92.61
	S3	96.12
GT2 PFCM	S1	92.70
	S2	94.21
	S3	97.24

TABLE IX: Confusion matrices and recognition rate for the best results in Type 1 PFCM, IT2 and GT-2 PFCM algorithms for Scene 1.

Algorithm	True Class \ Recognised Class	1	2	3	Recognition Rate
T1 PFCM	1	7693	57	470	89.90
	2	1549	22250	1647	
	3	318	0	6016	
IT2 PFCM	1	7551	374	295	90.73
	2	1334	22744	1368	
	3	286	50	5998	
GT2 PFCM	1	8065	155	6	92.70
	2	1270	22870	9	
	3	8	183	6143	

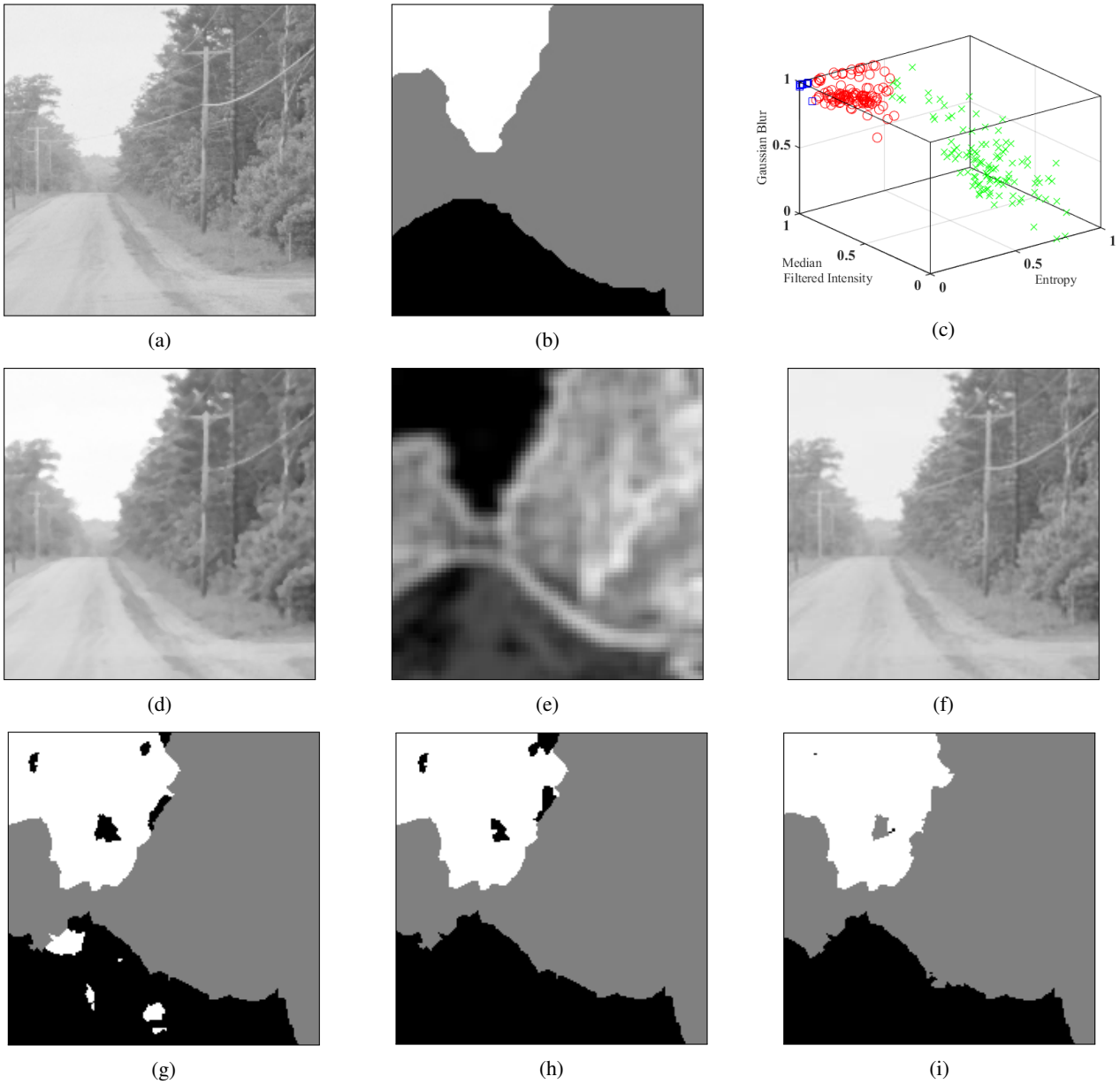

(a) (b) (c)

(d) (e) (f)

(g) (h) (i)

Fig. 11: Image segmentation for Scene 1: (a) original image, (b) mask image, (c) scatter plot of sample patterns, feature images of (d) median filtered intensity, (e) entropy, (f) Gaussian blur segmentation results for (g)T1-PFCM, (h) proposed IT2 PFCM, (i) proposed GT2 PFCM.

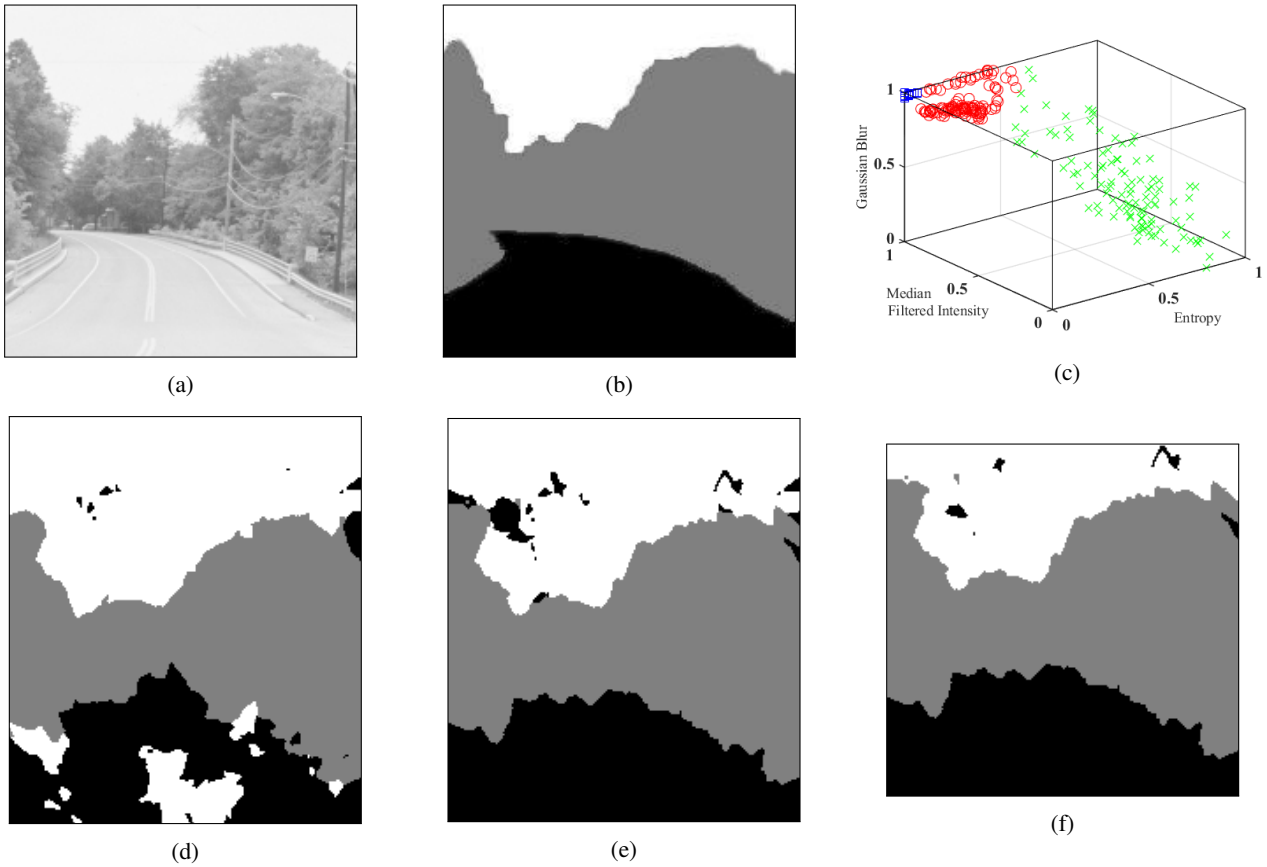

Fig. 12: Image segmentation for Scene 2: (a) original image, (b) mask image, (c) scatter plot of sample patterns, feature images of (d)T1-PFCM, (e) proposed IT2 PFCM, (f) proposed GT2 PFCM.

TABLE X: Confusion matrices and recognition rate for the best results in Type 1 PFCM, IT2 and GT-2 PFCM algorithms for Scene 2.

Algorithm	True Class \ Recognised Class	1	2	3	Recognition Rate
T1 PFCM	1	8423	348	2059	87.83
	2	923	17793	1135	
	3	274	129	8916	
IT2 PFCM	1	10603	227	0	92.61
	2	787	18522	542	
	3	778	622	7919	
GT2 PFCM	1	10603	227	0	94.21
	2	783	18522	546	
	3	168	591	8560	

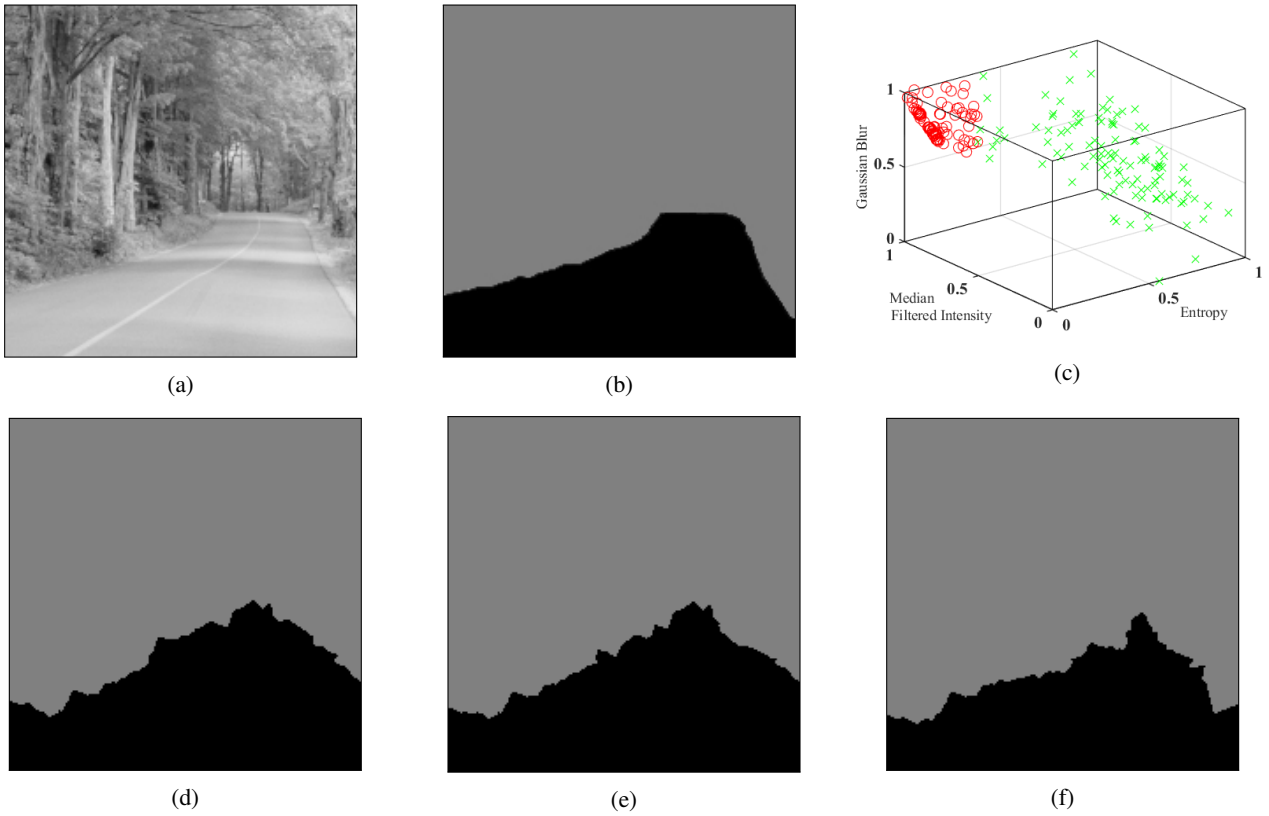

Fig. 13: Image segmentation for Scene 3: (a) original image, (b) mask image, (c) scatter plot of sample patterns, feature images of (d)T1-PFCM, (e) proposed IT2 PFCM, (f) proposed GT2 PFCM.

TABLE XI: Confusion matrices and recognition rate for the best results in Type 1 PFCM, IT2 and GT-2 PFCM algorithms for Scene 3.

Algorithm	Recognised Class / True Class	1	2	Recognition Rate
T1 PFCM	1	11316	176	
	2	1478	27030	95.87
IT2 PFCM	1	11143	349	
	2	1208	27300	96.12
GT2 PFCM	1	10579	913	
	2	190	28318	97.24

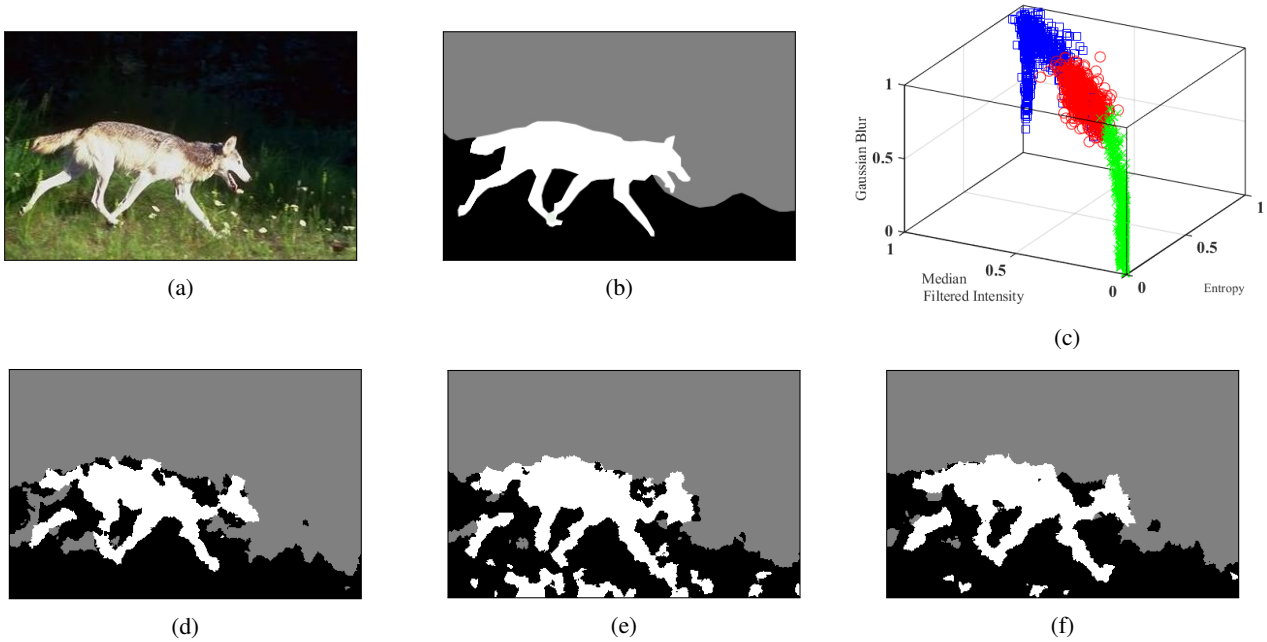

(a) (b) (c) (d) (e) (f)

Fig. 14: Image segmentation for Wolf Image: (a) original image, (b) mask image, (c) scatter plot of sample patterns, feature images of (d)T1-PFCM, (e) proposed IT2 PFCM, (f) proposed GT2 PFCM.

TABLE XII: Confusion matrices and recognition rate for the best results in Type 1 PFCM, IT2 and GT-2 PFCM algorithms for Wolf Image.

Algorithm	Recognised Class / True Class	1	2	3	Recognition Rate
T1 PFCM	1	22127	524	2785	89.57
	2	4325	46167	232	
	3	566	526	8652	
IT2 PFCM	1	21039	541	1622	89.35
	2	1815	45725	57	
	3	4164	951	9990	
GT2 PFCM	1	23688	675	1762	92.25
	2	1786	45793	145	
	3	1544	749	9762	

V. Conclusion

PFCM allows us to vary the constants a and b which in turn changes the contribution of FCM and PCM respectively. An interesting advantage of this is observed in dealing with datasets that have outlier points, where, the value of a can be taken comparatively less than that of b thereby increasing the effectiveness of PCM over FCM, similarly, in cases of datasets resulting in coincident clusters, contribution of FCM can be increased over PCM by taking a larger value of b as compared to a. Another importance of these manually changeable constants come to picture in case of random initialization of the cluster prototypes. The resulting clusters and hence the recognition rates depends on the initial choice of cluster centers. While an improvement in our proposed algorithm can be introduced by eliminating this dependency, maintaining a lower value of a reduces the same[26]. Further development in this course can be made in determining the optimal values of m_1, m_2, η_1 and η_2 depending on the datasets. Since our proposed algorithm tends to form spherical clusters, clustering of datasets like the spiral dataset[25] becomes difficult. In order to work on these datasets, path dependency in PFCM algorithm can be introduced.

Appendix A
Proof of the First Zonklar Equation

Appendix one text goes here.

APPENDIX B

Appendix two text goes here.

ACKNOWLEDGMENT

The project was conceptualized and completed at the Computational Vision and Fuzzy Systems Lab, Hanyang University.

REFERENCES

[1] P. Dayan, M. Sahani, and G. Deback, Unsupervised learning, *The MIT encyclopedia of the cognitive sciences,* 1999.
[2] M. Medynskaya, "Fuzzy set theory. the concept of fuzzy sets," in *Soft Computing and Measurements (SCM), 2015 XVIII International Conference on,* May 2015, pp. 3031.
[3] R.Suganya, R.Shanthi, "Fuzzy C- Means Algorithm- A Review," *International Journal of Scientific and Research Publications, Volume 2, Issue 11* pp. 440-442, 2012.
[4] Dongmei Han, Jiayu Ji, Yonghui Dai, Guowei Li, Weiguo Fan, Huagen Chen, " Improved Fuzzy C-Means Algorithm and Its Application to Classification of Remote Sensing Image in Chengdu City, China ," *International Conference on Progress in Informatics and Computing* pp. 437 - 443, 2016.
[5] Sudip Kumar Adhikari, Jamuna Kanta Sing, Dipak Kumar Basu, Mita Nasipuri, "A spatial fuzzy C-means algorithm with application to MRI image segmentation ," *Eighth International Conference on Advances in Pattern Recognition* pp. 1-6, 2015.
[6] Haifeng Yu, Junli Chen,Dinghu Qing, Shuiling Mao, Liang Liu, " An application of improved fuzzy C means clustering algorithm in tax administration," *IET International Communication Conference on Wireless Mobile and Computing* pp. 496 - 499, 2011.
[7] Zhiye Sun, Li Gao, Shuang Wei,Shijue Zheng, "A Fuzzy C-Means Clustering Algorithm and Application in Meteorological Data," *Second International Conference on Modeling, Simulation and Visualization Methods* pp. 15 - 18, 2010.
[8] P. Yugander, G. Raghotham Reddy, "Liver tumor segmentation in noisy CT images using distance regularized level set evolution based on fuzzy C-means clustering," *IEEE International Conference on Recent Trends in Electronics, Information & Communication Technology* pp. 1530 - 1534, 2017.
[9] Jin-Tsong Jeng, Chen-Chia Chuang, Sheng-Chieh Chang, "Interval fuzzy possibilistic c-means clustering algorithm on smart phone implement," *Proceedings of the SICE Annual Conference (SICE)* pp. 78 - 82, 2014.
[10] QiongdanHuang, LupingXu,"A method or radar targets position acquisition based on Possibilistic C_means algorithm," *CIE International Conference on Radar* pp. 1 - 4, 2006.
[11] Qingchen Zhang, Laurence T. Yang, Zhikui Chen, Feng Xia,"A High-Order Possibilistic C-Means Algorithm for Clustering Incomplete Multimedia Data," *IEEE Systems Journal Volume 11, Issue 4* pp. 2160 - 2169, 2017.
[12] Qingchen Zhang, Laurence T. Yang, Zhikui Chen, Peng Li,"PPHOPCM: Privacy-preserving High-order Possibilistic c-Means Algorithm for Big Data Clustering with Cloud Computing," *IEEE Transactions on Big Data (Early Access)* pp. 1 - 1, 2017.
[13] Zhenping Xie, Shitong Wang, F. L. Chung,"An enhanced possibilistic C-Means clustering algorithm EPCM," *Soft Computing vol.12, no. 6,* pp 593611, 2008.
[14] N.R. Pal, K. Pal, J.C. Bezdek, "A mixed c-means clustering model," *Proceedings of 6th International Fuzzy Systems Conference vol.1,* pp 11 - 21 , 1997.
[15] N.R. Pal, K. Pal, J.M. Keller, J.C. Bezdek, "A possibilistic fuzzy c-means clustering algorithm," *IEEE Transactions on Fuzzy Systems vol. 13, no. 4,* pp 517 - 530, 2005.
[16] C. Hwang and F. C.-H. Rhee, "Uncertain Fuzzy Clustering: Interval Type-2 Fuzzy Approach to C-Means," *IEEE Transactions on Fuzzy Systems vol.15, no. 1,* pp 107 - 120 , 2007.
[17] Ji-Hee Min, Eun-A Shim and Frank Chung-Hoon Rhee, "An interval type-2 fuzzy pcm algorithm for pattern recognition," *IEEE International Conference on Fuzzy Systems,* pp 480 - 483 , 2009.
[18] Jerry M. Mendel, "General Type-2 Fuzzy Logic Systems Made Simple: A Tutorial," *IEEE Transactions on Fuzzy Systems vol. 22, no. 5,* pp 1162 - 1182 , 2014.
[19] Liang Zhao, Yanzhen Li and Yanjun Li, "Computing with Words for Discrete General Type-2 Fuzzy Sets Based on α Plane," *Proceedings of 2013 IEEE International Conference on Vehicular Electronics and Safety,* pp 268-272 , 2013.
[20] Feilong Liu, "An efficient centroid type-reduction strategy for general type-2 fuzzy logic system," *Information SciencesInformatics and Computer Science, Intelligent Systems, Applications: An International Journal vol. 178, no. 9,* pp 2224-2236 , 2008.
[21] Ondrej Linda and Milos Manic, "General Type-2 Fuzzy C-Means Algorithm for Uncertain Fuzzy Clustering," *IEEE Transactions on Fuzzy Systems vol. 20, no. 5,* pp 883 - 897 , 2012.
[22] J.M. Mendel and R.I.B. John, "Type-2 fuzzy sets made simple," *IEEE Transactions on Fuzzy Systems vol. 10, no. 2,* pp 117 - 127 , 2002.
[23] Yang Chen and Dazhi Wang, "Studies on Centroid Type-reduction Algorithms for Interval Type-2 Fuzzy Logic Systems," *IEEE Fifth International Conference on Big Data and Cloud Computing,* pp 344 - 349 , 2015.
[24] Jerry M. Mendel, "Comments on "α -Plane Representation for Type-2 Fuzzy Sets: Theory and Applications," *IEEE Transactions on Fuzzy Systems vol. 18, no. 1,* pp 229 - 230 , 2009.
[25] D. Dua and E. Karra Taniskidou, Uci machine learning repository, 2017.
[26] Zengfeng Wang, "Comparison of Four Kinds of Fuzzy C-Means Clustering Methods," *Third International Symposium on Information Processing,* pp 563 - 566, 2010.

PLACE PHOTO HERE

Michael Shell Biography text here.

John Doe Biography text here.

Jane Doe Biography text here.